# Enzymatic Mechanism of Human Apurinic/Apyrimidinic Endonuclease against a THF AP Site Model Substrate†

Sophia T. Mundle,‡ James C. Delaney,§ John M. Essigmann,§ and Phyllis R. Strauss*,‡

*Department of Biology, Northeastern University, Boston, Massachusetts 02115, and Departments of Biological Engineering and Chemistry, Massachusetts Institute of Technology, Cambridge, Massachusetts 02139*

*Received August 26, 2008; Revised Manuscript Received November 10, 2008*

ABSTRACT: The endonucleolytic activity of human apurinic/apyrimidinic endonuclease (AP endo) is a major factor in the maintenance of the integrity of the human genome. There are estimates that this enzyme is responsible for eliminating as many as $10^5$ potentially mutagenic and genotoxic lesions from the genome of each cell every day. Furthermore, inhibition of AP endonuclease may be effective in decreasing the dose requirements of chemotherapeutics used in the treatment of cancer as well as other diseases. Therefore, it is essential to accurately and directly characterize the enzymatic mechanism of AP endo. Here we describe specifically designed double-stranded DNA oligomers containing tetrahydrofuran (THF) with a 5′-phosphorothioate linkage as the abasic site substrate. Using $H_2{}^{18}O$ during the cleavage reaction and leveraging the stereochemical preferences of AP endo and T4 DNA ligase for phosphorothioate substrates, we show that AP endo acts by a one-step associative phosphoryl transfer mechanism on a THF-containing substrate.



Human apurinic/apyrimidinic endonuclease (AP endo,[1] HAP1, Apex, Ref1) is a DNA base excision repair enzyme with a wide variety of functions, including AP endonuclease [cleaving an AP site 5′ to a deoxyribose phosphate (dRP) moiety], 3′ exonuclease, 3′ phosphodiesterase, 3′ phosphatase, RNaseH, and 5′ endonuclease activities (reviewed in refs *1* and *2*). The characterization of the human enzyme occurred several years after the *Escherichia coli* functional homologue (ExoIII) was found to have AP endonuclease activity (*3*−*10*). In addition to the wide variety of functions, mammalian AP endo has been shown to act on many types of DNA substrate molecules but demonstrates the most robust activity when acting as a class II AP endonuclease. The turnover number for 5′ cleavage of a reduced AP site is 10 $s^{-1}$ (*11*), even faster than the highly effective DNA repair enzyme uracil DNA glycosylase (UDG), which has a turnover number for uracil excision of 5 $s^{-1}$ (*12*).

A variety of AP site analogues have been tested in probing the 5′ AP site nicking activity of AP endo (*11*, *13*−*15*). Of particular interest here is the fact that replacement of a nonbridging phosphorus oxygen 5′ to the AP site with sulfur has major consequences on enzymatic activity. In 1995, Wilson et al. showed that incision activity on the $S_p$ isomer of a phosphorothioate by the human AP endo is 10000-fold reduced while incision on the $R_p$ isomer is only 20-fold reduced (*14*). Therefore, in a mixture of $S_p$ and $R_p$ stereoisomers of AP endo substrate, the enzyme will have a vast preference for cleavage of the $R_p$ stereoisomer.

We recently proposed a two-step enzymatic mechanism in which $Tyr^{171}$ acts directly as the attacking nucleophile (*16*). One way to evaluate this proposal involves use of substrate DNA containing a phosphorothioate linkage. Phosphorothioate RNA and DNA have been used in a wide variety of applications [reviewed by Summerton (*17*)], including RNA-mediated interference (RNAi) (*18*) and as drugs targeted toward specific pathogenic proteins, as in the case of the malarial topoisomerase II (*19*). By far, the most specific use of phosphorothioate oligonucleotides has been in the investigation of the stereochemical course of enzymatic reactions (*20*−*23*).

DNA cleavage reactions performed on phosphorothioate DNA in the presence of $H_2{}^{18}O$ generate product DNA with a 5′ terminal chiral thiophosphate (*21*). The chirality of the product DNA is dependent on both the stereochemistry of the starting material ($S_p$ or $R_p$) and the nature of the enzymatic reaction (one-step reaction with inversion of configuration of the scissile phosphate or two-step reaction, which occurs with no net inversion of configuration). Product DNA generated in this manner can then be configurationally defined using the well-documented stereochemistry of the T4 DNA ligase reaction, through which the *pro-R* oxygen from the 5′ terminal thiophosphate donor is always lost to AMP during the course of the ligase reaction (*21*) (Figure 1). Knowing that T4 DNA ligase is able to ligate DNA efficiently when a 5′ dRP group is present at the terminus of the donor DNA (*24*) enabled us to follow the fate of $^{18}O$ after AP endo cleavage of the $R_p$ stereoisomer of substrate DNA, and subsequent ligation of the product DNA with a partner oligonucleotide. We could thus discriminate between

† Supported by National Institutes of Health Grant CA 72702 (to P.R.S.) and NIH Grant CA80024 and NIEHS Grant P30 ES002109 (to J.M.E.).

* To whom correspondence should be addressed. Telephone: (617) 373-3492. Fax: (617) 373-2138. E-mail: p.strauss@neu.edu.

‡ Northeastern University.

§ Massachusetts Institute of Technology.

[1] Abbreviations: AP endo, apurinic/apyrimidinic endonuclease; AP, abasic; BER, base excision repair; dRP, deoxyribose phosphate; ESI-TOF MS, electrospray ionization time-of-flight mass spectrometry; THF, tetrahydrofuran.

10.1021/bi8016137 CCC: $40.75 
Published on Web 12/10/2008

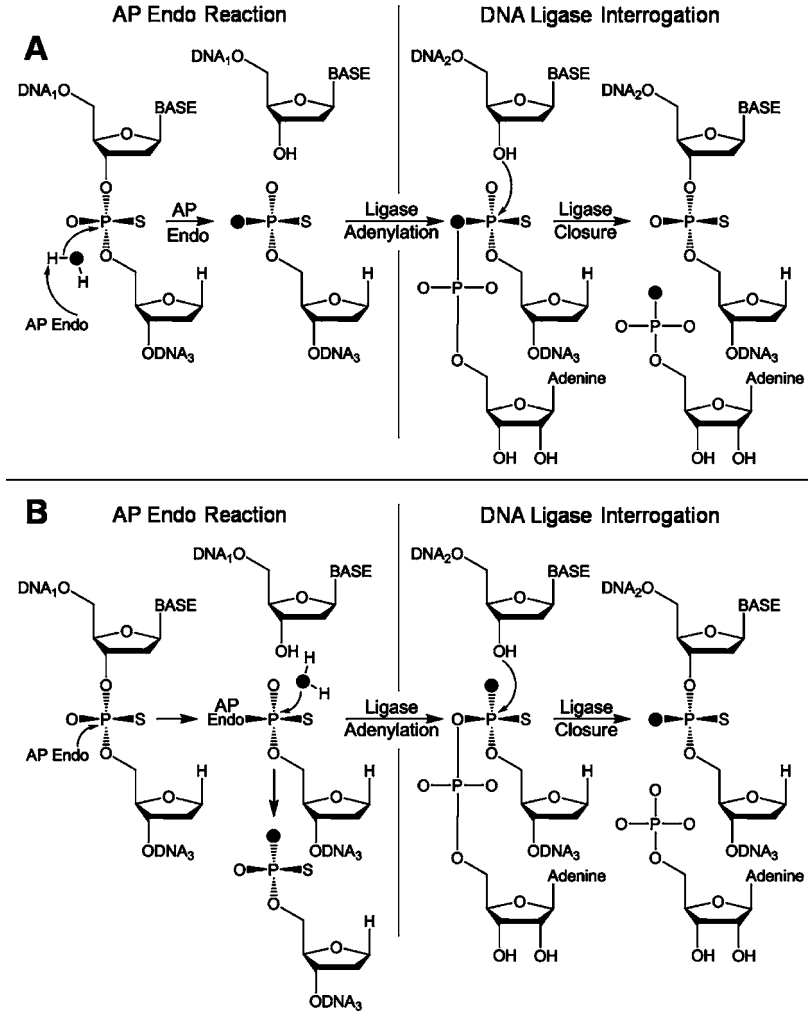


FIGURE 1: Stereochemical course of the reactions described in the text. Panel A shows the fate of $^{18}O$ (●) in a one-step hydrolytic mechanism. Panel B shows the fate of $^{18}O$ (●) in a two-step hydrolytic mechanism. Since it is known that AP endonuclease appreciably cleaves only the $R_p$ diastereomer, the reaction is depicted using the $R_p$ stereoisomer as the starting material. In a one-step hydrolysis, $^{18}O$ is transferred to the *pro-R* oxygen of the cleaved oligomer product but is then lost to AMP during the stereospecific T4 DNA ligase reaction (*58*). In a two-step hydrolysis, the heavy oxygen is transferred to the *pro-S* oxygen of the cleaved product DNA and is retained during the stereospecific T4 DNA ligase reaction. Bond order and charge about the phosphorus were omitted for the sake of stereochemical clarity.



a one-step (Figure 1A) and a two-step (Figure 1B) hydrolytic mechanism.

## EXPERIMENTAL PROCEDURES

Three oligonucleotides were designed such that the AP endo reaction site or ligation site was flanked by *Hae*III restriction sites (underlined). The tetrahydrofuran AP site analogue containing a 5′ phosphorothioate linkage is represented by sF, while the analogous phosphodiester control is abbreviated as pF: STM5, 5′ CCATGCCTGCACGAsFTGGCCGAATTCTTC 3′; STM6, 5′ GAAGAATTCGGCCAGTCGTGCAGGCATGG 3′; and STM7, 5′ GAAGAATTCGGCCAGAGGCCAAGAGCGCGCTTTTGCGCGCTCTTGGCCT 3′.

These oligomers were synthesized Trityl-OFF by GeneLink (Hawthorne, NY). DNA oligonucleotide STM5 was generated by automated DNA synthesis (Expedite 8909 DNA Synthesizer, PerSeptive Biosystems, Inc., Framingham, MA) and standard phosphoramidite chemistry. The phosphorothioate linkage was introduced using the Beaucage (*25*) sulfurizing reagent (3*H*-1,2-benzodithiol-3-one 1,1-dioxide) (Glen Research, Sterling, VA), which yields ~96% phosphorothioate linkages. The stable AP site (THF, F) was introduced into the DNA oligomer using dSpacer CE phosphoramidite {5′-*O*-dimethoxytrityl-1′,2′-dideoxyribose-3′-[(2-cyanoethyl)(*N*,*N*-diisopropyl)]phosphoramidite} (Glen Research). Attempts to resolve the $S_p$ and $R_p$ diastereomers by HPLC using reversed-phase columns and the many conditions described by Subach et al. (*26*) for our sequences were unsuccessful. Therefore, the AP endo reaction was performed on a mixture of diastereomers. DNA samples were PAGE-purified from an 18% preparative gel. All oligomers were greater than 95% pure as determined by 5′ $^{32}P$ end labeling with polynucleotide kinase (New England Biolabs, Beverly, MA), resolution on an 18% denaturing polyacrylamide gel, and PhosphorImager analysis. After PAGE purification, desalted oligomers were dissolved in either sterile $H_2O$ or sterile $H_2{}^{18}O$ (Cambridge Isotope Laboratories, Inc., Cambridge, MA). The subsequent enzymatic reactions were performed in either 100% $H_2O$ or $H_2{}^{18}O$ (at 96% isotopic abundance).

The overall experimental scheme is depicted in Figure 2. The substrate for the AP endo reaction was generated by annealing STM5 and STM6 in equimolar quantities (final DNA concentration of 4 $\mu$M). This was accomplished by

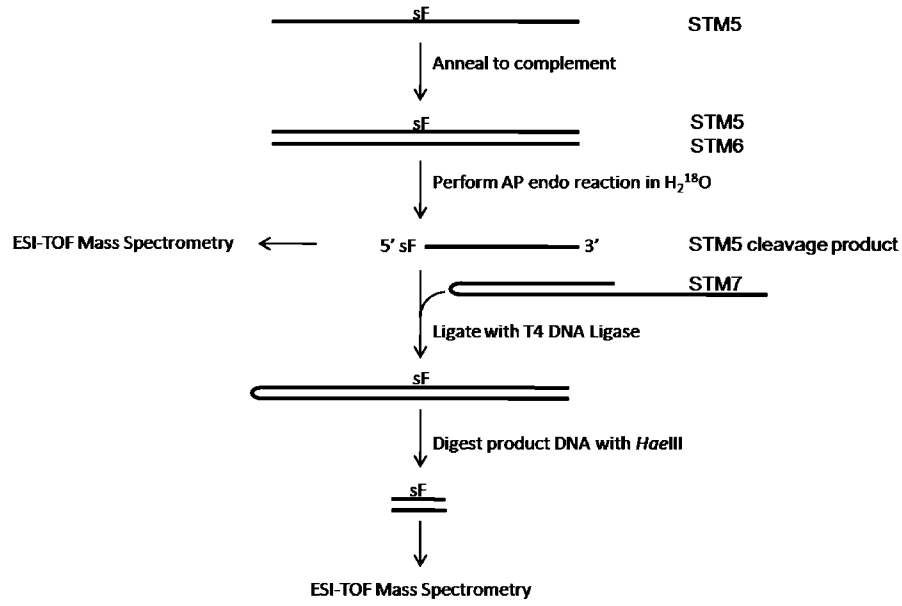


FIGURE 2: Schematic representation of the phosphorothioate experiment to determine the AP endo reaction mechanism. sF represents the tetrahydrofuran AP site analogue containing a 5′ phoshorothioate linkage, and analysis of ESI-TOF mass spectra was performed using the extracted ions of the modified single-stranded DNA.

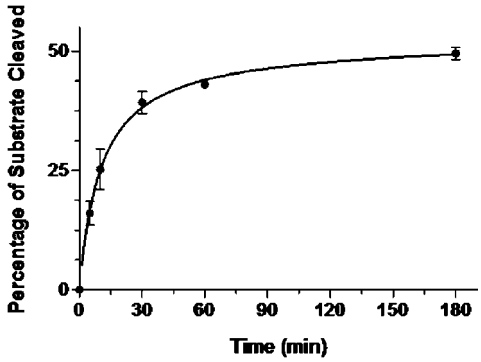


FIGURE 3: Time course of the AP endo reaction. The ability of AP endo to cleave the constructed substrate DNA was examined using radiolabeled substrate DNA and conditions as described in the text. These data are the average of two independent experiments, each point being determined in duplicate in each experiment.

heating the mixture to 70 °C and allowing it to cool slowly to room temperature in either $H_2O$ or $H_2{}^{18}O$. The mixture for the AP endo reaction, performed in a total volume of 800 $\mu$L, contained 750 nM double-stranded substrate DNA and 100 nM AP endo in 50 mM Hepes/NaOH (pH 7.5), 0.1 mM EDTA, 65 mM NaCl, 10% glycerol, and 5 mM $MgCl_2$. Initially, a time course (0−3 h) was performed using a total reaction volume of 5 $\mu$L and 5′ $^{32}$P end-labeled substrate DNA, which determined that 3 h was an appropriate end point for the reaction (Figure 3). Reaction mixtures were incubated for 3 h at 22 °C, and then reactions were terminated by addition of EDTA to a final concentration of 100 mM. The reaction mixture was desalted using illustra MicroSpin G-25 columns (GE Healthcare, Buckinghamshire, U.K.), phenol-extracted, and ethanol-precipitated in the presence of 0.3 M sodium acetate. To ensure that $^{18}$O was incorporated into the reaction product, a sample was analyzed by mass spectrometry as described in Results.

Following processing of the AP endo reaction product, all subsequent steps were performed in sterile, nonisotopically enriched $H_2O$. Ligation reactions were performed in a total volume of 100 $\mu$L. Eight thousand picomoles (≈8-fold molar ratio) STM7 hairpin DNA was mixed with the AP endo reaction product. The DNA mixture was heated to 70 °C and slow-cooled to room temperature for annealing. The samples were then allowed to cool to 16 °C for 5 min before addition of T4 DNA ligase buffer (ATP included) and 60 units of T4 DNA ligase (Promega Corp., Madison, WI). After ligation reaction mixtures had been incubated for 2 h at 16 °C, an additional 60 units of T4 DNA ligase and 50 nmol of fresh ATP were added. Ligation reactions were allowed to proceed overnight at 16 °C. The T4 DNA ligase reaction product was processed by G-25 desalting. The sample was then digested with 80 units of *Hae*III (New England Biolabs) in 120−130 $\mu$L of 1× NE buffer 2 for 2−4 h at 37 °C followed by heat inactivation of the enzyme at 80 °C for 20 min. Analysis of 100 $\mu$L of the *Hae*III product was then performed by electrospray ionization time-of-flight mass spectrometry (ESI-TOF MS) by means of an Agilent 1100 MSD ESI-TOF instrument calibrated with a commercial tuning mixture just prior to analysis [as in the Supplementary Methods of Delaney et al. (*27*) with some minor modifications to the HPLC method].

ESI-TOF MS afforded the extreme sensitivity and isotopic resolution required to differentiate between $^{16}$O and $^{18}$O in a 7mer single-stranded DNA molecule. Mass accuracy and resolution were typically less than 1 ppm and higher than 10000, respectively. The following parameters were used: capillary voltage of −3500 V, nebulizing gas pressure of 35 psi, and drying gas flow of 12 L/min at 325 °C. The fragmentor was set at 225 V, and scans were taken from *m*/*z* 100 to 2000. The injection needle was washed twice in 100% methanol prior to injection of the sample onto the column. An Agilent 1100 Series thermostated autosampler in series with a reverse-phase column (Agilent Zorbax SB-Aq, 3.5 $\mu$m, 2.1 mm × 150 mm) was used to introduce the sample at 0.3 mL/min, using a gradient from 0 to 50% B over 20 min followed by a gradient from 50 to 80% B over 5 min, and equilibration from 0 to 0% B for 12 min (A, 10 mM ammonium acetate; B, 100% acetonitrile). The time of

entry into the mass spectrometer for the 15mer AP endo product was 9.4 min and for the 7mer AP endoligated/*Hae*III product 8.1 min. The expected monoisotopic values for the most populated charge states of a given single-stranded DNA fragment of interest were used to extract the ions from the total ion chromatograph; a range of 4 *m*/*z* centered about the expected $^{16}O$ monoisotopic value was used, ensuring representation of both $^{16}O$ and $^{18}O$ species. The background was subtracted from the appropriate extracted ion peak, taking juxtaposed regions of identical width from both sides.

## RESULTS

Initial experiments were performed to determine suitable conditions for the AP endo reaction. After varying the concentration of the enzyme and the amount of time that the reaction was allowed to proceed, we determined that at 750 nM substrate and 100 nM enzyme, a reaction time of 3 h was sufficient to convert most, if not all, of the $R_p$ substrate DNA into product. Figure 3 represents the time course of the AP endo reaction. By 3 h, the rate of the reaction had tapered off, and the amount of product was ~50% of the amount of substrate. This result indicated that the reaction had gone to completion and that cleavage of the $S_p$ diastereomer was minimal. Confirmation of the report that AP endo cleaves the $R_p$ stereoisomer (*14*) was obtained by digestion of the AP endo reaction product with either nuclease P1 (which cleaves the $S_p$ stereoisomer and not $R_p$) or snake venom phosphodiesterase (which cleaves the $R_p$ stereoisomer and not $S_p$). Analysis of these products by ESI-TOF MS confirmed that the DNA refractory to cleavage by AP endo was also resistant to cleavage by snake venom phosphodiesterase but sensitive to cleavage by nuclease P1, as predicted (see the Supporting Information).

The T4 DNA ligase reaction was optimized using $^{32}P$ end-labeled substrate DNA. The ratio of AP endo reaction product to STM7 49mer hairpin oligomers was varied. Product formation was maximal with an 8:1 ratio of STM7 acceptor to 5′ thiophosphate donor DNA and by addition of extra ATP (0.5 mM) and ligase (60 units) midreaction, as described by Carey et al. (*28*). Although only 1−3% ligation occurred (data not shown), the quantity of product (80−240 pmol) was sufficient for detection by ESI-TOF MS. Consequently, the reaction was scaled up and performed without the radiolabel (see below). The experiment was designed to eliminate the need for purification of oligonucleotide fragments after each enzymatic step, which would have been an arduous task. As judged by mass spectrometry of the AP endo product and its ligation/*Hae*III product, the 29mer starting material contained ~5% of a 5′ phosphodiester−THF (pF) linkage [16 amu less than the expected phosphorothioate product (data not shown)]. This outcome could be possible due to incomplete sulfurization or desulfurization during solid-phase chemical synthesis (*29*, *30*), and the difficulty of purifying a large DNA molecule. Since the ligation efficiency of the AP endo cleavage product was low (1−3%), one may be concerned that most of the ligated material would be from the pF contaminant, which would presumably ligate more efficiently. This possibility was not the case, as there was ~5% of the pF signal for both the 15mer AP endo product and the 7mer ligation/*Hae*III product. Nevertheless, the small pF contaminant did not adversely affect the mass

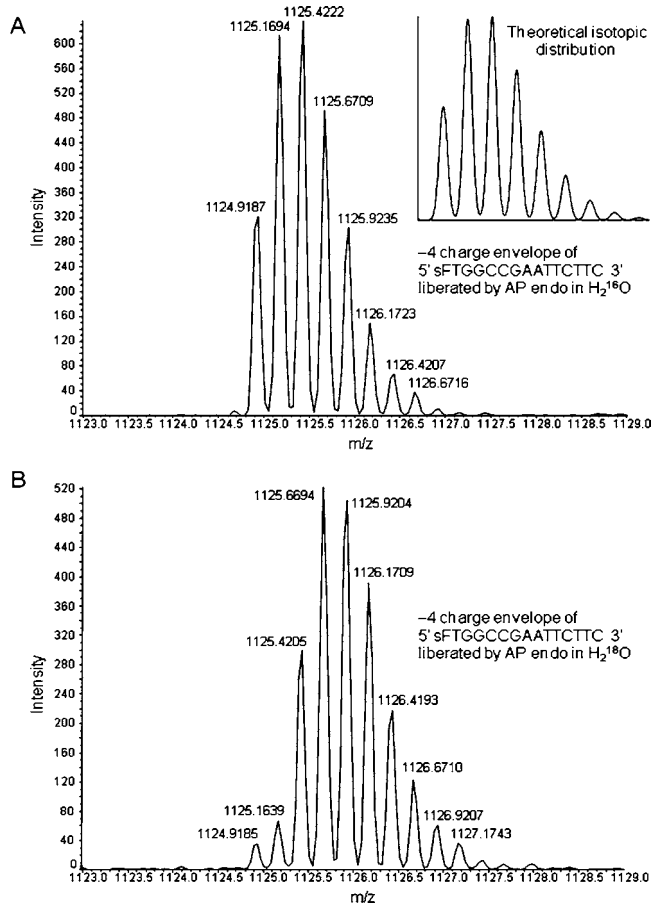


FIGURE 4: ESI-TOF MS analysis of the AP endonuclease reaction product performed in $H_2O$ and $H_2{}^{18}O$. ESI-TOF MS was performed as described in Experimental Procedures. Panel A shows the results obtained when the AP endo reaction was performed in $H_2O$, as well as the theoretical isotopic distribution. Panel B shows the results of the AP endo reaction performed in $H_2{}^{18}O$. Extraction of ions between *m*/*z* 1123 and 1127 revealed −4 envelopes containing monoisotopic (100% $^{12}C$) values of *m*/*z* 1124.919 (reaction in $H_2O$) and 1125.421 (reaction in $H_2{}^{18}O$) for the single-stranded 15mers. The theoretical isotopic distribution for 5′ sFTGGCCGAATTCTTC 3′ is shown in the inset.

spectral interpretation, since our analysis focused on molecules that contained the phosphorothioate linkage, and ligation of the AP endo product to a dissimilar oligonucleotide ensured that the observed events occurred from a successful AP endo event (allowing $^{18}O$ incorporation), followed by a successful T4 DNA ligase event.

To determine whether the modified conditions for ESI-TOF MS used by Delaney et al. (*27*) were appropriate for this DNA sample, we analyzed the AP endo reaction product prior to ligation. The expected molecular formula for the neutral 15mer AP endo reaction product bearing the 5′ sF group in $H_2O$ is $C_{141}H_{184}N_{47}O_{92}P_{15}S_1$, which has a theoretical monoisotopic (100% $^{12}C$) mass to charge ratio (*m*/*z*) of 1124.916 in the −4 charge state. After analysis of the sample and extraction of ions at *m*/*z* 1123−1127, a characteristic mass spectrum for DNA of the appropriate size (*m*/*z* 1124.919) was obtained (Figure 4A). Despite ion extraction, the signal for the −3 charge state (*m*/*z* 1500.224) was poorly resolved, and that for the −5 charge state (*m*/*z* 899.731) was not detected (data not shown). Molecular Weight Calculator version 6.45, written by M. Monroe for the U.S. Department of Energy (under Grant RR018522 and Contract DE-AC05-

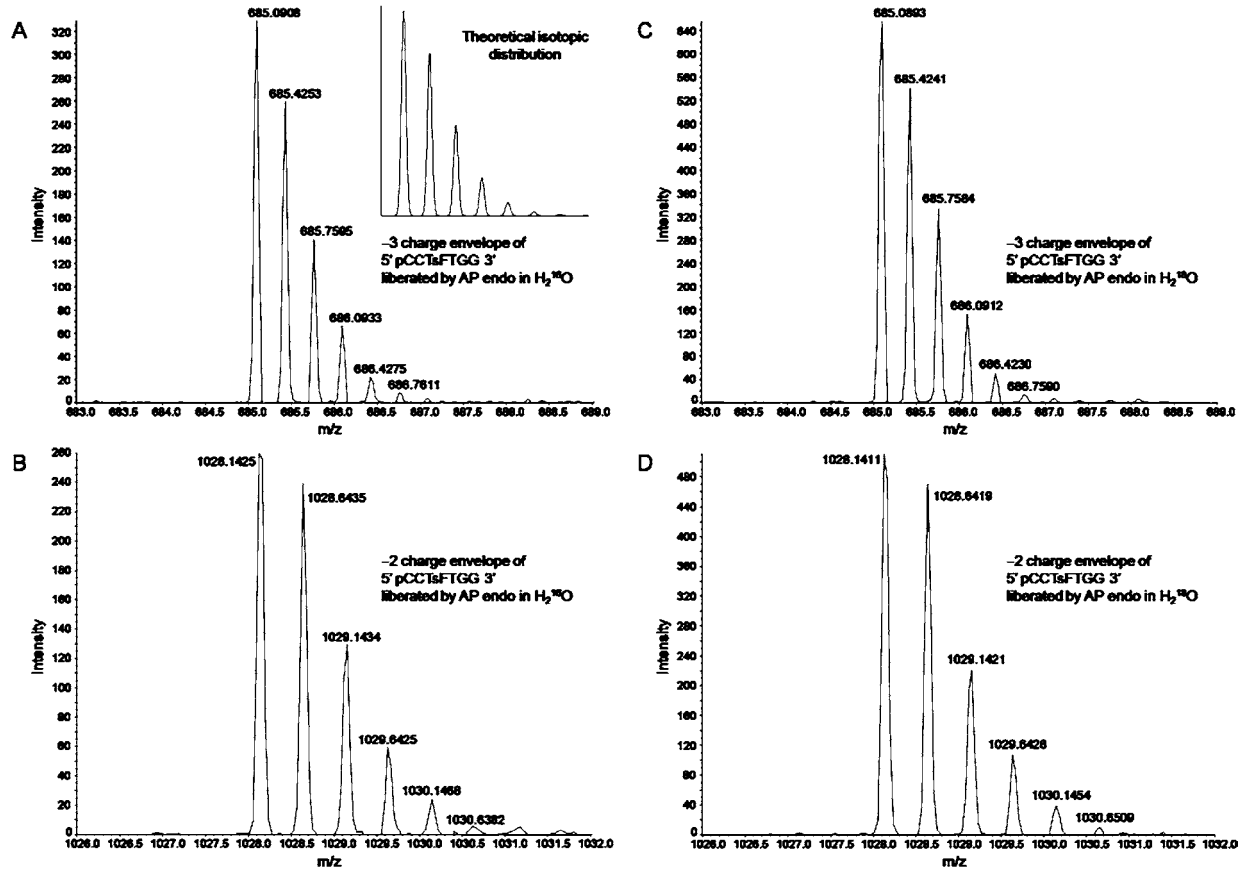


FIGURE 5: ESI-TOF MS analysis of the ligation/*Hae*III reaction product performed in $H_2O$. ESI-TOF MS was performed as described in the text. Mass to charge ratios of the single-stranded 7mer were obtained for the −3 [*m*/*z* 685.091 (A)] and −2 [*m*/*z* 1028.143 (B)] charge states. The theoretical isotopic distribution for 5′ pCCTsFTGG 3′ (any charge state) is shown in the inset. Mass to charge ratios of the single-stranded 7mer product DNA were similar to those obtained when the AP endo reaction was performed in $H_2O$ for the −3 [*m*/*z* 685.089 (C)] and −2 [*m*/*z* 1028.141 (D)] charge states. This result indicates that the reaction proceeds by a one-step mechanism.



76RL0 1830, Pacific Northwest National Laboratory, Richland, WA) revealed that the theoretical isotopic distribution (Figure 4A, inset) agreed well with what was observed. The signal for the −4 charge state was strong enough to rationalize performance of the large-scale reaction with unlabeled substrate in $H_2{}^{18}O$ for analysis of products. In $H_2{}^{18}O$, the expected molecular formula for the neutral product DNA is $C_{141}H_{184}N_{47}O_{91}P_{15}S_1 + {}^{18}O_1$, which has a theoretical *m*/*z* ratio of 1125.417 in the −4 charge state. Upon extraction of *m*/*z* 1123−1127 ions, a signal at *m*/*z* 1125.421 was obtained (Figure 4B). Minor (<15%) contamination with the $^{16}O$ product DNA was expected since there was ∼4−5% $H_2O$ present during the reaction, which has no bearing on the analysis, as the complete retention versus complete loss of $^{18}O$ signal is probed (and not $^{18}O$:$^{16}O$ ratios). These results served as proof of principal, in that we were able to demonstrate incorporation of $H_2{}^{18}O$ into the AP endo reaction product and that the $^{18}O$ signal was sufficiently abundant to discern its retention versus loss.

The product of the AP endo reaction in $H_2O$, followed by ligation and *Hae*III digestion, is expected to be a 7mer with a neutral molecular formula of $C_{63}H_{85}N_{20}O_{43}P_7S_1$ and monoisotopic *m*/*z* ratios of 685.091 and 1028.140 in the −3 and −2 charge states, respectively. After extraction of ions from *m*/*z* 683 to 687 and from *m*/*z* 1026 to 1030, we found close agreement of the theoretical with the observed *m*/*z* values of 685.093 and 1028.143 (Figure 5A,B). The Molecular Weight Calculator revealed that the theoretical isotopic distribution agreed well with what was observed for the −3 charge state (Figure 5A); the small increased deviation in the *m*/*z* 1028.6 peak for the −2 charge state (Figure 5B) is most likely due to a species comigrating on this rather steep LC gradient. In the case of a one-step hydrolysis, the *m*/*z* ratios of the AP endo reaction product performed in $H_2{}^{18}O$, followed by ligation and *Hae*III digestion, were expected to be the same as when they were performed in $H_2O$ (Figure 5A,B). In the event of a two-step hydrolysis, $^{18}O$ incorporation would give a neutral molecular formula of $C_{63}H_{85}N_{20}O_{42}P_7S_1 + {}^{18}O_1$ and expected *m*/*z* ratios of 685.759 and 1029.142 for the −3 and −2 charge states, respectively. Panels C and D of Figure 5 show that the *m*/*z* ratios obtained after reaction in $H_2{}^{18}O$ of 685.089 and 1028.141 for the −3 and −2 charge states, respectively, correlated well with the values seen when the reaction was performed in $H_2O$, even though $^{18}O$ had clearly been incorporated into the starting material prior to ligation. Therefore, we conclude that AP endo cleaves a THF-containing substrate by a one-step mechanism.

## DISCUSSION

Here, we describe experiments, using mass spectrometry, $H_2{}^{18}O$, and the known stereochemical preferences of AP endo and T4 DNA ligase, that determine the enzymatic mechanism of human AP endo, a critical enzyme in maintaining the integrity of the human genome during normal metabolism

as well as in times of oxidative stress. Phosphorothioate-containing DNA oligomers are a powerful tool for studying the stereochemistry of DNA-metabolizing enzymes involved in phosphoryl transfer reactions (reviewed in refs *31* and *32*). In particular, they have been used to determine the type of mechanism employed by a number of restriction endonucleases (*21, 22, 33*−*39*), vaccinia type 1 topoisomerase (*23*), DNA polymerase I Klenow fragment (*40*), and HIV-1 reverse transcriptase (*41*−*43*), among others.

Enzymes that cleave the phosphodiester backbone of DNA molecules generally act by one of two mechanisms, which differ in the identity of the nucleophile that carries out the attack. The most common mechanism is one in which activated water is the attacking nucleophile. In this one-step mechanism, a highly unstable pentacoordinate transition state is formed, resulting in cleavage of the scissile bond. Most type II restriction endonucleases act by this type of mechanism (*21, 33*−*39*). The less common two-step mechanism is one in which a nucleophile, provided by the enzyme, carries out direct attack of the scissile phosphate. In a two-step mechanism, nucleophilic attack results in the formation of a covalent intermediate between the enzyme and the DNA. This intermediate is displaced by water, resulting in cleavage of the scissile bond. Members of the phospholipase D family of enzymes act by a two-step mechanism, in which a covalent phosphohistidine intermediate is formed (*44*−*47*). Both one-step (*48*−*51*) and two-step (*16*) mechanisms have been proposed for the AP endo mechanism of action. We were particularly interested in the chemical mechanism of AP endo in deciphering the role of $Tyr^{171}$ at the active site (*16*) and because of the physiological importance of this enzyme (*52*−*54*). Additionally, understanding the chemistry of an enzyme is an essential tool in the design of inhibitors, which in this case could be used in concomitant therapy to increase the dose effectiveness of cancer chemotherapeutics (*52*−*56*). Most chemotherapeutics act by damaging DNA, with the resulting damage often being repaired by DNA repair enzymes, such as AP endo. Therefore, if DNA repair can be inhibited in actively dividing cells, and the most actively dividing cells are cancer cells in most cases, then the dose of chemotherapeutic agents might be reduced without losing efficacy.

The Strauss laboratory published the first single-turnover studies of AP endo and determined explicit binding and dissociation kinetics (*11*). We also have shown that both $His^{309}$ and $Tyr^{171}$ are intimately involved in catalysis by this enzyme (*15, 16*). Recently, Maher and Bloom published the first pre-steady state kinetic analysis of cleavage of a THF-containing substrate (*57*). They showed that the cleavage rate of AP endo is so fast that it is immeasurable using stopped-flow kinetics (minimally 850 $s^{-1}$). The most important conclusion from the latter study (which investigated the wild type as well as H309N and D210A mutants) is the fact that a slow step, which occurs after chemistry but before dissociation, limits the steady state incision activity to 2−10 $s^{-1}$. The authors suggest a conformational change, which occurs after cleavage of the DNA, resulting in the following minimal enzymatic scheme:

$$E + S \leftrightarrow [ES] \rightarrow [EP] \rightarrow [EP^*] \rightarrow E + P$$

On the basis of the results presented here, the most likely mechanism for AP endo on a THF-containing substrate is an associative one-step hydrolytic mechanism. An analysis of the active site (Figure 6) implicates $His^{309}$ as the general base generating the attacking nucleophile, with $Tyr^{171}$ most likely acting as a guide to properly position the THF-containing substrate for catalysis. We suggest the following mechanism for human AP endo, when acting on a THF-containing substrate: Binding of substrate DNA and the required divalent cation renders the enzyme catalytically "active". Although the divalent cation does not make direct contact with $Tyr^{171}$, it does perturb the molecular environment of this residue (S. T. Mundle et al., manuscript in preparation). This perturbation, in turn, allows $Tyr^{171}$ to properly position the AP site for cleavage. $Mg^{2+}$, which is liganded by $Glu^{96}$, makes contact with a nonbridging oxygen of the scissile phosphate, rendering it electropositive and open to attack, presumably by water. $His^{309}$ generates the attacking nucleophile. Attack results in the formation of a pentavalent transition state, followed by expulsion of the 5′ leaving group and cleavage of the phosphodiester bond.

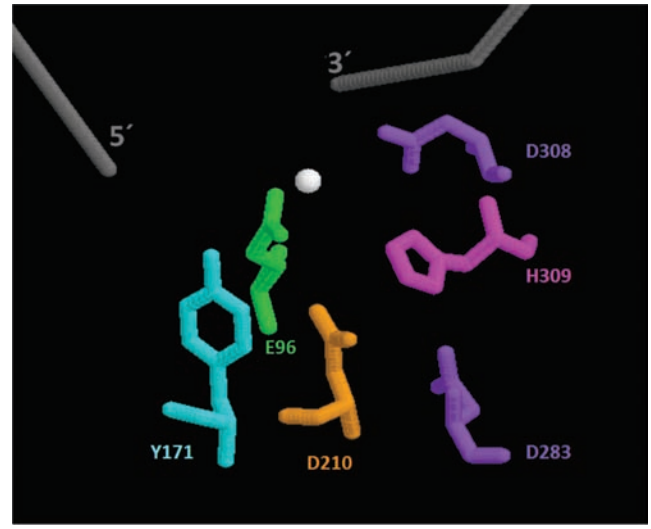


FIGURE 6: Stereoview showing the active site residues of human AP endo in complex with cleaved product DNA (*50*). The proposed roles of active site residues, $His^{309}$ (magenta), $Tyr^{171}$ (cyan), and $Glu^{96}$ (green), are described in the text. $Glu^{96}$ is shown bound to the divalent cation ($Mn^{2+}$) (white), with which the structure was cocrystallized. Others (*50*) have proposed that $Asp^{210}$ (orange) may serve to generate the attacking nucleophile. Lucas et al. (*15*) have shown that, on the basis of kinetic studies, both $Asp^{283}$ and $Asp^{308}$ (purple), which flank the active site histidine, are equally involved in maintaining the conformation of the active site. This figure was created using the RasMol molecular viewing program (*59*).

In this study, we expand upon evidence that AP endo cleaves the $R_p$ but not the $S_p$ stereoisomer of DNA phosphorothioate oligomers, albeit slowly with respect to a phosphodiester substrate (*14*). This observation was important to the overall scheme of the work presented here. Since separation of the $R_p$ and $S_p$ diastereomers of the substrate DNA was not achieved, the AP endo reaction was performed on a substrate which contained a 1:1 mixture of the two. In the $S_p$ diastereomer of phosphorothioate DNA, sulfur occupies what would be the *pro-S* oxygen of a phosphodiester linkage; therefore, the $S_p$ diastereomer sterically prevents binding by the required divalent cation, $Mg^{2+}$, which under normal circumstances makes contact with the nonbridging *pro-S* oxygen of the phosphodiester bond, ensuring that AP endo is only able to cleave the $R_p$-containing substrate molecule. Here we show unequivocally that the mechanism

of AP endo on a THF-containing substrate DNA proceeds by a one-step mechanism, which has always been shown to proceed with inversion of configuration at the scissile phosphate.

## SUPPORTING INFORMATION AVAILABLE

Additional experimental procedures and results, evidence that the material analyzed in this study was derived from AP endo selectively cleaving the *R* phosphorothioate isomer (Figure S1), evidence that AP endo shows a vast preference for cleavage of the $R_p$ stereoisomer versus the $S_p$ stereoisomer (Figure S2), and analysis of the free G nitrogenous base that indicates that more than half the amount of DNA from the nuclease P1 digest was analyzed, with respect to the snake venom phosphodiesterase digest (Figure S3). This material is available free of charge via the Internet at http://pubs.acs.org.

## REFERENCES


1. Evans, A. R., Limp-Foster, M., and Kelley, M. R. (2000) Going APE over ref-1. *Mutat. Res. 461*, 83–108.
2. Strauss, P. R., and O'Regan, N. E. (2001) Abasic Site Repair in Higher Eukaryotes. In *DNA Damage and Repair* (Nickoloff, J. A., and Hoekstra, M. F., Eds.) pp 43−85, Humana Press Inc., Totowa, NJ.
3. Yajko, D. M., and Weiss, B. (1975) Mutations simultaneously affecting endonuclease II and exonuclease III in *Escherichia coli*. *Proc. Natl. Acad. Sci. U.S.A. 72*, 688–692.
4. Linsley, W. S., Penhoet, E. E., and Linn, S. (1977) Human endonuclease specific for apurinic/apyrimidinic sites in DNA. Partial purification and characterization of multiple forms from placenta. *J. Biol. Chem. 252*, 1235–1242.
5. Mosbaugh, D. W., and Linn, S. (1980) Further characterization of human fibroblast apurinic/apyrimidinic DNA endonucleases. The definition of two mechanistic classes of enzyme. *J. Biol. Chem. 255*, 11743–11752.
6. Rogers, S. G., and Weiss, B. (1980) Exonuclease III of *Escherichia coli* K-12, an AP endonuclease. *Methods Enzymol. 65*, 201–211.
7. Robson, C. N., and Hickson, I. D. (1991) Isolation of cDNA clones encoding a human apurinic/apyrimidinic endonuclease that corrects DNA repair and mutagenesis defects in *E. coli* xth (exonuclease III) mutants. *Nucleic Acids Res. 19*, 5519–5523.
8. Robson, C. N., Milne, A. M., Pappin, D. J., and Hickson, I. D. (1991) Isolation of cDNA clones encoding an enzyme from bovine cells that repairs oxidative DNA damage in vitro: Homology with bacterial repair enzymes. *Nucleic Acids Res. 19*, 1087–1092.
9. Seki, S., Akiyama, K., Watanabe, S., Hatsushika, M., Ikeda, S., and Tsutsui, K. (1991) cDNA and deduced amino acid sequence of a mouse DNA repair enzyme (APEX nuclease) with significant homology to *Escherichia coli* exonuclease III. *J. Biol. Chem. 266*, 20797–20802.
10. Seki, S., Ikeda, S., Watanabe, S., Hatsushika, M., Tsutsui, K., Akiyama, K., and Zhang, B. (1991) A mouse DNA repair enzyme (APEX nuclease) having exonuclease and apurinic/apyrimidinic endonuclease activities: Purification and characterization. *Biochim. Biophys. Acta 1079*, 57–64.
11. Strauss, P. R., Beard, W. A., Patterson, T. A., and Wilson, S. H. (1997) Substrate binding by human apurinic/apyrimidinic endonuclease indicates a Briggs-Haldane mechanism. *J. Biol. Chem. 272*, 1302–1307.
12. Slupphaug, G., Eftedal, I., Kavli, B., Bharati, S., Helle, N. M., Haug, T., Levine, D. W., and Krokan, H. E. (1995) Properties of a recombinant human uracil-DNA glycosylase from the UNG gene and evidence that UNG encodes the major uracil-DNA glycosylase. *Biochemistry 34*, 128–138.
13. Erzberger, J. P., Barsky, D., Scharer, O. D., Colvin, M. E., and Wilson, D. M. (1998) Elements in abasic site recognition by the major human and *Escherichia coli* apurinic/apyrimidinic endonucleases. *Nucleic Acids Res. 26*, 2771–2778.
14. Wilson, D. M., III, Takeshita, M., Grollman, A. P., and Demple, B. (1995) Incision activity of human apurinic endonuclease (Ape) at abasic site analogs in DNA. *J. Biol. Chem. 270*, 16002–16007.
15. Lucas, J. A., Masuda, Y., Bennett, R. A., Strauss, N. S., and Strauss, P. R. (1999) Single-turnover analysis of mutant human apurinic/apyrimidinic endonuclease. *Biochemistry 38*, 4958–4964.
16. Mundle, S. T., Fattal, M. H., Melo, L. F., Coriolan, J. D., O'Regan, N. E., and Strauss, P. R. (2004) Novel role of tyrosine in catalysis by human AP endonuclease 1. *DNA Repair 3*, 1447–1455.
17. Summerton, J. E. (2007) Morpholino, siRNA, and S-DNA compared: Impact of structure and mechanism of action on off-target effects and sequence specificity. *Curr. Top. Med. Chem. 7*, 651–660.
18. Rocchi, P., Jugpal, P., So, A., Sinneman, S., Ettinger, S., Fazli, L., Nelson, C., and Gleave, M. (2006) Small interference RNA targeting heat-shock protein 27 inhibits the growth of prostatic cell lines and induces apoptosis via caspase-3 activation in vitro. *BJU Int. 98*, 1082–1089.
19. Foger, F., Noonpakdee, W., Loretz, B., Joojuntr, S., Salvenmoser, W., Thaler, M., and Bernkop-Schnurch, A. (2006) Inhibition of malarial topoisomerase II in *Plasmodium falciparum* by antisense nanoparticles. *Int. J. Pharm. 319*, 139–146.
20. Elliott, S. L., Brazier, J., Cosstick, R., and Connolly, B. A. (2005) Mechanism of the *Escherichia coli* DNA T:G-mismatch endonuclease (Vsr protein) probed with thiophosphate-containing oligodeoxynucleotides. *J. Mol. Biol. 353*, 692–703.
21. Mizuuchi, K., Nobbs, T. J., Halford, S. E., Adzuma, K., and Qin, J. (1999) A new method for determining the stereochemistry of DNA cleavage reactions: Application to the SfiI and HpaII restriction endonucleases and to the MuA transposase. *Biochemistry 38*, 4640–4648.
22. Sasnauskas, G., Connolly, B. A., Halford, S. E., and Siksnys, V. (2007) Site-specific DNA transesterification catalyzed by a restriction enzyme. *Proc. Natl. Acad. Sci. U.S.A. 104*, 2115–2120.
23. Stivers, J. T., Jagadeesh, G. J., Nawrot, B., Stec, W. J., and Shuman, S. (2000) Stereochemical outcome and kinetic effects of Rp- and Sp-phosphorothioate substitutions at the cleavage site of vaccinia type I DNA topoisomerase. *Biochemistry 39*, 5561–5572.
24. Bogenhagen, D. F., and Pinz, K. G. (1998) The action of DNA ligase at abasic sites in DNA. *J. Biol. Chem. 273*, 7888–7893.
25. Iyer, R. P., Egan, W., Regan, J. B., and Beaucage, S. L. (1990) 3H-1,2-Benzodithiol-3-one 1,1-dioxide as an improved sulfurizing reagent in the solid-phase synthesis of oligodeoxyribonucleoside phosphorothioates. *J. Am. Chem. Soc. 112*, 1253–1254.
26. Subach, F. V., Müller, S., Tashlitsky, V. N., Petrauskene, O. V., and Gromova, E. S. (2003) The preparation of DNA duplexes containing internucleotide phosphorothioate groups in various positions of the recognition site for the EcoRII restriction endonuclease. *Russ. J. Bioorg. Chem. 29*, 566–573.
27. Delaney, J. C., Smeester, L., Wong, C., Frick, L. E., Taghizadeh, K., Wishnok, J. S., Drennan, C. L., Samson, L. D., and Essigmann, J. M. (2005) AlkB reverses etheno DNA lesions caused by lipid oxidation in vitro and in vivo. *Nat. Struct. Mol. Biol. 12*, 855–860.
28. Carey, D. C., and Strauss, P. R. (1999) Human apurinic/apyrimidinic endonuclease is processive. *Biochemistry 38*, 16553–16560.
29. Cieslak, J., Ausin, C., Chmielewski, M. K., Kauffman, J. S., Snyder, J., Del-Grosso, A., and Beaucage, S. L. (2005) $^{31}$P NMR study of the desulfurization of oligonucleoside phosphorothioates effected by "aged" trichloroacetic acid solutions. *J. Org. Chem. 70*, 3303–3306.
30. Xu, Q., Barany, G., Hammer, R. P., and Musier-Forsyth, K. (1996) Efficient introduction of phosphorothioates into RNA oligonucleotides by 3-ethoxy-1,2,4-dithiazoline-5-one (EDITH). *Nucleic Acids Res. 24*, 3643–3644.
31. Eckstein, F. (1985) Nucleoside phosphorothioates. *Annu. Rev. Biochem. 54*, 367–402.
32. Knowles, J. R. (1980) Enzyme-catalyzed phosphoryl transfer reactions. *Annu. Rev. Biochem. 49*, 877–919.
33. Connolly, B. A., Eckstein, F., and Pingoud, A. (1984) The stereochemical course of the restriction endonuclease EcoRI-catalyzed reaction. *J. Biol. Chem. 259*, 10760–10763.
34. Connolly, B. A., Potter, B. V., Eckstein, F., Pingoud, A., and Grotjahn, L. (1984) Synthesis and characterization of an octanucleotide containing the EcoRI recognition sequence with a phosphorothioate group at the cleavage site. *Biochemistry 23*, 3443–3453.
35. Grasby, J. A., and Connolly, B. A. (1992) Stereochemical outcome of the hydrolysis reaction catalyzed by the EcoRV restriction endonuclease. *Biochemistry 31*, 7855–7861.

36. Jeltsch, A., Alves, J., Wolfes, H., Maass, G., and Pingoud, A. (1993) Substrate-assisted catalysis in the cleavage of DNA by the EcoRI and EcoRV restriction enzymes. *Proc. Natl. Acad. Sci. U.S.A. 90*, 8499–8503.
37. Koziolkiewicz, M., and Stec, W. J. (1992) Application of phosphate-backbone-modified oligonucleotides in the studies on EcoRI endonuclease mechanism of action. *Biochemistry 31*, 9460–9466.
38. Nobbs, T. J., Williams, S. A., Connolly, B. A., and Halford, S. E. (1998) Phosphorothioate substrates for the SfiI restriction endonuclease. *Biol. Chem. 379*, 599–604.
39. Thorogood, H., Grasby, J. A., and Connolly, B. A. (1996) Influence of the phosphate backbone on the recognition and hydrolysis of DNA by the EcoRV restriction endonuclease. A study using oligodeoxynucleotide phosphorothioates. *J. Biol. Chem. 271*, 8855–8862.
40. Dahlberg, M. E., and Benkovic, S. J. (1991) Kinetic mechanism of DNA polymerase I (Klenow fragment): Identification of a second conformational change and evaluation of the internal equilibrium constant. *Biochemistry 30*, 4835–4843.
41. El Dirani-Diab, R., Sarih-Cottin, L., Delord, B., Dumon, B., Moreau, S., Toulme, J. J., Fleury, H., and Litvak, S. (1997) Phosphorothioate oligonucleotides derived from human immunodeficiency virus type 1 (HIV-1) primer tRNALys3 are strong inhibitors of HIV-1 reverse transcriptase and arrest viral replication in infected cells. *Antimicrob. Agents Chemother. 41*, 2141–2148.
42. Kaushik, N., Rege, N., Yadav, P. N., Sarafianos, S. G., Modak, M. J., and Pandey, V. N. (1996) Biochemical analysis of catalytically crucial aspartate mutants of human immunodeficiency virus type 1 reverse transcriptase. *Biochemistry 35*, 11536–11546.
43. Radzio, J., and Sluis-Cremer, N. (2005) Stereo-selectivity of HIV-1 reverse transcriptase toward isomers of thymidine-5′-O-1-thiotriphosphate. *Protein Sci. 14*, 1929–1933.
44. Gottlin, E. B., Rudolph, A. E., Zhao, Y., Matthews, H. R., and Dixon, J. E. (1998) Catalytic mechanism of the phospholipase D superfamily proceeds via a covalent phosphohistidine intermediate. *Proc. Natl. Acad. Sci. U.S.A. 95*, 9202–9207.
45. Interthal, H., Pouliot, J. J., and Champoux, J. J. (2001) The tyrosyl-DNA phosphodiesterase Tdp1 is a member of the phospholipase D superfamily. *Proc. Natl. Acad. Sci. U.S.A. 98*, 12009–12014.
46. Ponting, C. P., and Kerr, I. D. (1996) A novel family of phospholipase D homologues that includes phospholipid synthases and putative endonucleases: Identification of duplicated repeats and potential active site residues. *Protein Sci. 5*, 914–922.
47. Waite, M. (1999) The PLD superfamily: Insights into catalysis. *Biochim. Biophys. Acta 1439*, 187–197.
48. Beernink, P. T., Segelke, B. W., Hadi, M. Z., Erzberger, J. P., Wilson, D. M., III, and Rupp, B. (2001) Two divalent metal ions in the active site of a new crystal form of human apurinic/apyrimidinic endonuclease, Ape1: Implications for the catalytic mechanism. *J. Mol. Biol. 307*, 1023–1034.
49. Gorman, M. A., Morera, S., Rothwell, D. G., de La Fortelle, E., Mol, C. D., Tainer, J. A., Hickson, I. D., and Freemont, P. S. (1997) The crystal structure of the human DNA repair endonuclease HAP1 suggests the recognition of extra-helical deoxyribose at DNA abasic sites. *EMBO J. 16*, 6548–6558.
50. Mol, C. D., Izumi, T., Mitra, S., and Tainer, J. A. (2000) DNA-bound structures and mutants reveal abasic DNA binding by APE1 and DNA repair coordination [corrected]. *Nature 403*, 451–456.
51. Oezguen, N., Schein, C. H., Peddi, S. R., Power, T. D., Izumi, T., and Braun, W. (2007) A "moving metal mechanism" for substrate cleavage by the DNA repair endonuclease APE-1. *Proteins 68*, 313–323.
52. Fishel, M. L., and Kelley, M. R. (2007) The DNA base excision repair protein Ape1/Ref-1 as a therapeutic and chemopreventive target. *Mol. Aspects Med. 28*, 375–395.
53. Luo, M., and Kelley, M. R. (2004) Inhibition of the human apurinic/apyrimidinic endonuclease (APE1) repair activity and sensitization of breast cancer cells to DNA alkylating agents with lucanthone. *Anticancer Res. 24*, 2127–2134.
54. Robertson, K. A., Bullock, H. A., Xu, Y., Tritt, R., Zimmerman, E., Ulbright, T. M., Foster, R. S., Einhorn, L. H., and Kelley, M. R. (2001) Altered expression of Ape1/ref-1 in germ cell tumors and overexpression in NT2 cells confers resistance to bleomycin and radiation. *Cancer Res. 61*, 2220–2225.
55. Fahrig, R., Quietzsch, D., Heinrich, J. C., Heinemann, V., Boeck, S., Schmid, R. M., Praha, C., Liebert, A., Sonntag, D., Krupitza, G., and Hanel, M. (2006) RP101 improves the efficacy of chemotherapy in pancreas carcinoma cell lines and pancreatic cancer patients. *Anti-Cancer Drugs 17*, 1045–1056.
56. Yang, Z. Z., Chen, X. H., and Wang, D. (2007) Experimental study enhancing the chemosensitivity of multiple myeloma to melphalan by using a tissue-specific APE1-silencing RNA expression vector. *Clin. Lymphoma Myeloma 7*, 296–304.
57. Maher, R. L., and Bloom, L. B. (2007) Pre-steady-state kinetic characterization of the AP endonuclease activity of human AP endonuclease 1. *J. Biol. Chem. 282*, 30577–30585.
58. Engler, M. J., and Richardson, C. C. (1982) The Enzymes. In *The Enzymes* (Boyer, P. D., Ed.) pp 3−29, Academic Press, New York.
59. Sayle, R. A., and Milner-White, E. J. (1995) RASMOL: Biomolecular graphics for all. *Trends Biochem. Sci. 20*, 374.

BI8016137